Astron. Astrophys. 325, 1163–1173 (1997)

ASTRONOMY
AND
ASTROPHYSICS

A 330-360 GHz spectral survey of G 34.3+0.15

II. Chemical modelling⋆

T.J. Millar[1], **G.H. Macdonald**[2], **and A.G. Gibb**[2]

[1] Department of Physics, UMIST, P.O. Box 88, Manchester, M60 1QD, UK
[2] Electronic Engineering Laboratory, University of Kent, Canterbury, Kent CT2 7NT, UK

Received 12 September 1996 / Accepted 21 February 1997

Abstract. We describe a detailed depth- and time-dependent model of the molecular cloud associated with the ultracompact H II region G 34.3+0.15. Previous work on observations of NH_3 and CS indicates that the molecular cloud has three distinct physical components:- an ultracompact hot core, a compact hot core and an extended halo. We have used the physical parameters derived from these observations as input to our detailed chemical kinetic modelling. The results of the model calculations are discussed with reference to the different chemistries occuring in each component and are compared with abundances derived from our recent spectral line survey of G 34.3+0.15 (Paper I).

Key words: ISM: individual objects: G 34.3+0.15 – ISM: molecules – ISM: abundances

1. Introduction

Hot molecular cores are small, dense hot clumps of gas in star-forming regions. They show anomalously large abundances of several species including small hydrogenated molecules such as NH_3 and H_2S, large molecules such as ethanol, C_2H_5OH, and dimethyl ether, $(CH_3)_2O$, and much larger deuterium fractionation than expected for their measured gas kinetic temperatures, around 100 – 250 K. It is now accepted that the chemical evolution of hot cores is related to the evaporation of grain mantle material, material which has been both accreted and synthesised on grains before the switch-on of a nearby star initiated sublimation.

Although early models of hot core chemistry incorporated both the cold accretion phase and the high-temperature phase (Brown et al. 1988; Brown & Millar 1989a,b), more recent models have concentrated on the hot phase by assuming as initial conditions high abundances of small saturated species and following their subsequent gas-phase chemistry (Millar et al. 1991; Charnley et al. 1992; Caselli et al. 1993; Charnley & Millar 1994; MacKay 1995; Charnley et al. 1995). Such an approach reflects the current uncertainty in how one should model grain chemistry. On the other hand, this approach may enable conclusions to be drawn about the solid-state chemistry; Millar et al. (1995) have argued that their observation of ethanol in G 34.3 implies that it must be synthesised on the grains.

To date, chemical modelling of hot molecular cores has concentrated on 'one-point' models in which one set of physical parameters is adopted (density, temperature, initial grain mantle abundances, etc.) and the time-dependent chemical evolution of the hot core gas followed.

In parallel with the development of theoretical models, there have been a number of molecular line surveys of hot core regions, including those in Sgr B2 (Turner 1991; Sutton et al. 1991), Orion (Sutton et al. 1995), W3 (Helmich & van Dishoeck 1997) and G 34.3+0.15 (Macdonald et al. 1996). The distance and physical complexity of the Sgr B2 cloud has prevented any detailed chemical modelling, while the hot cores in Orion have been studied theoretically (Charnley et al 1992; Caselli et al 1993). One-point models for the W3 sources, which include one hot core, have also been constructed (Helmich et al. 1997). However, the physical structure of the molecular cloud associated with G 34.3 is well known from observations of NH_3 (Heaton et al. 1989), HCO^+ (Heaton et al. 1993), CS (Hauschildt et al. 1995) and CI/CO (Little et al. 1994), making it the only hot molecular core for which a depth-dependent model can be constructed. Although the hot cores in Orion and Sgr B2 have been observed with high spatial resolution, these sources have a much more complex spatial structure than is obvious from the current observations of G 34.3 and which precludes detailed modelling at the present time. The observations of G 34.3+0.15 all indicate a three-component structure to the molecular cloud surrounding the ultracompact H II region. Our recent 330 – 360 GHz spectral survey of this cloud detected 338 spectral lines from at least 35 distinct chemical species, and rotation diagrams were constructed for 13 species to determine abundances and rota-

Send offprint requests to: T.J. Millar

⋆ Tables 5 and 6 and Figs. 1-3, 5 and 6 are only available in electronic form at the CDS via anonymous ftp to cdsarc.u-strasbg.fr (130.79.128.5) or via http://cdsweb.u-strasbg.fr/Abstract.html

Table 1. Physical parameters adopted in the model. The radial distance, r, is measured in pc.

Component	$n(H_2)$ (cm^{-3})	T (K)	Outer radius (pc)	$N(H_2)$ (cm^{-2})	A_V (mag)
Ultracompact core	$2\ 10^7$	300	0.01	$6\ 10^{23}$	640
Compact core	10^6	$30r^{-0.4}$	0.1	$2.7\ 10^{23}$	288
Halo	$10^4 r^{-2}$	$30r^{-0.4}$	3.5	$2.9\ 10^{23}$	310

Table 2. Initial abundances with respect to total H nuclei in the chemical model of the compact cores

Species	Abundance	Species	Abundance	Species	Abundance
H^+	$1\ 10^{-10}$	He^+	$2.5\ 10^{-11}$	H_3^+	$1\ 10^{-8}$
CO	$5\ 10^{-5}$	CH_4	$2\ 10^{-7}$	H_2CO	$4\ 10^{-8}$
C_2H_2	$5\ 10^{-7}$	CH_3OH	$5\ 10^{-7}$	C_2H_4	$5\ 10^{-9}$
C_2H_6	$5\ 10^{-9}$	N_2	$2\ 10^{-5}$	NH_3	$1\ 10^{-5}$
O_2	$1\ 10^{-6}$	H_2O	$1\ 10^{-5}$	H_2S	$1\ 10^{-6}$
Si^+	$3.6\ 10^{-8}$	Fe^+	$2.4\ 10^{-8}$		

tion temperatures. Lower limits to abundances were found for many other species (Macdonald et al. 1996, hereafter Paper I). The results showed evidence that contributions to line emission arise in each of the three components of the cloud, sometimes all three for a particular species. To aid in the interpretation of the physical and chemical evolution of the G 34.3 molecular cloud, we have used the three component model to describe the chemistry and to compare the results of model calculations to the observations of Paper I. In Sect. 2, we describe the physical and chemical model adopted, Sect. 3 presents the results, with a discussion of the chemistries in each cloud component and of specific molecules and comparision with observations, and conclusions and suggestions for future work in Sect. 4.

2. Description of the model

2.1. The physical model

Our model for the density and temperature distribution is taken from Heaton et al. (1989), based on VLA mapping of NH_3, and HCO^+ observations by Heaton et al. (1993). They have identified a hot ultracompact core (UCC) within a radius less than 0.025 pc and $n(H_2) = 2\ 10^7$ cm^{-3}, a compact core (CC) with a radius of about 0.1 pc and a density of 10^6 cm^{-3}, surrounded by a massive halo extending out to 3.5 pc with a H_2 density which falls off as r^{-2} (Little et al. 1994). Similar values are derived from the CS observations of Hauschildt et al. (1995). The detailed parameters are given in Table 1, where we have used the relationship A_V = 1.6 magnitudes per kpc per H-atom to convert $N(H_2)$ to A_V. One can see from the large values of A_V that photoreactions should not be important in determining the chemical evolution of the bulk of the gas in G 34.3. This conclusion may not be valid if the cloud is very clumpy close to the ultracompact H II region, although the lack of radicals and ions - which can be readily generated by photons - indicates that UV photons are not capable of penetrating the bulk of the cloud very effectively.

2.2. The chemical model

The physical structure of G 34.3 is such that it is likely that the components have undergone a different chemical evolution. The standard picture for hot molecular cores, which should apply to the ultracompact and compact cores, is that material in the hot core has been evaporated from grain surfaces by some heating event. The gas-phase chemical evolution of these regions is thus determined primarily by the material evaporated from the grains, the temperature of the gas and, to a lesser extent, the density (Rodgers & Millar 1996). On the other hand, the halo of the cloud, which is much cooler and less dense, has evolved from atomic gas. In these calculations we have neglected any possible dynamical evolution of the halo gas, although of course one should couple both the chemical and dynamical evolutions. The reasons for the neglect are that chemical-dynamical models generally have to adopt some free-fall, or pseudo-free fall, collapse, which may not be the case, and that this adds a degree of complexity which is unnecessary for this first attempt at a detailed depth-dependent model. Dynamical effects may need to be included in future models, particularly if outflows play a major role in the dynamical evolution of the gas in hot cores. To facilitate modelling of these different environments, we have constructed a reaction network which includes both evolution from atomic gas and from species evaporated from grain mantles. This network contains 225 species and 2184 reactions.

We have calculated time-dependent models at 22 radial points, 2 in the ultracompact core, 2 in the compact core and 18 in the halo, the few number of points in the cores being the result of almost constant physical conditions there. Each model is run over 10^8 years and has density and temperatures set by the parameters in Table 1. The initial conditions of the models differ. In the two cores, the initial state of the gas is molecular although there is some residual ionisation caused by cosmic rays. Initial fractional abundances given in Table 2. These are based on hot core models of other sources (Charnley et al. 1992; Charnley et al. 1995; Helmich et al. 1997). For the halo, we assume all elements, with the exception of hydrogen, which we take to be molecular, are in atomic form, with total abundances given by summing the relevant abundances of the species in the cores. Our calculation is self-consistent in that we assume that all gas-phase heavy elements get accreted onto the mantles of grains in the high density cores where they are converted to molecules which eventually evaporate under the influence of a nearby young star.

Our output consists of molecular abundances over a period of 10^8 years for each of the 22 depth points. However, it is clear that not all combinations of results can be used in the model. For example, the time-scale for evolution of the cores must be

Table 3. Activation energy barrier in degrees kelvin for the reactions of neutral parent species with atomic hydrogen. The data are taken from the NIST database (Mallard et al. 1994).

Species	E_A	Species	E_A	Species	E_A
CO	77700	CH_4	4045	H_2CO	1650
C_2H_2	11200	CH_3OH	2450	C_2H_4	6160
C_2H_6	3730	N_2	71000	NH_3	4990
O_2	8460	H_2O	9720	H_2S	352

less than that of the halo. We have thus looked for best fits to the observational data, which give integrated column densities through all three components, by combining abundances at one time in the evolution of the cores with the abundances at another time in the halo. The calculations give abundances per unit volume and we have integrated over depth to calculate column densities in each component and through the whole cloud.

Thus, we are able to follow the chemical evolution of each component through following the fractional abundances, whilst using column densities to find the times at which the models best fit the observations. In addition, because we calculate column densities in each component, we can see where the major contribution to column density occurs. In a complex source such as G 34.3, this is not always clear from a rotation diagram analysis.

3. Results

Before discussing the results of individual species, we begin this section by outlining the main chemical processes at work in each of the three components. This analysis is based on a large number of calculated models. The reader may find it instructive to refer to Figs. 1 to 6, which will be discussed in more detail later in the paper.

3.1. The physical components

3.1.1. The ultracompact core

This is the densest and warmest part of the molecular cloud. At $t = 0$, molecular ices are evaporated into a 300 K gas. Two important classes of reaction break down evaporated molecules:- (i) reactions with atomic hydrogen, and (ii) reactions with protonated molecules. Some small loss occurs also by cosmic-ray-induced photons. For most parent molecules, H-atom reactions have appreciable activation energy barriers which are listed in Table 3. The H-atoms primarily arise through the cosmic-ray ionisation of H_2 (55%), although a significant fraction is also produced in the reaction of radicals such as OH with H_2 (25 %), and by dissociative recombination of protonated ions such as NH_4^+ and H_3O^+ (20 %). At early times, around 1000 yr, loss of H occurs mainly through reaction with species such as NH_2 and CH_2 and leads to a fractional abundance of around 5×10^{-6}.

It can be seen from this Table that of the parent molecules, H_2S possesses the smallest barrier and will therefore be destroyed quickly by hydrogen atoms in the ultracompact core. Fig. 1 shows the evolution of the column densities within the UCC component as a function of time. It can be seen that the initial H_2S abundance is reduced by more than an order of magnitude within 1000 years and the released sulphur processed into SO via the S + O_2 reaction. Once SO forms, the SO_2 abundance increases rapidly. The rapid destruction of H_2S and consequent rise of SO and SO_2 is a strong function of temperature - cooler 'hot cores' will have more H_2S than warmer cores - and Charnley (1997) has proposed that if the gas temperature is known, observations of the sulphur-bearing species may be used to place constraints on the ages of hot cores.

For other parent molecules, reactions with H atoms are slow and proton transfer reactions of neutrals with H_3^+ and ionic reactions with H^+ and He^+ liberate reactive atoms and radicals from the parents, as well as form associated ions. This can be seen in Fig. 1 for NH_3 which does not decrease until 10^4 yr. Within 1000 years after evaporation, neutral-neutral reactions lead to the formation of HCN, HNC and HC_3N amongst others, whilst ion-neutral reactions build larger molecules such as acetaldehyde, CH_3CHO, ketene, CH_2CO, methyl formate, $HCOOCH_3$, and dimethyl ether, $(CH_3)_2O$. The abundances of ethanol, C_2H_5OH, and acetone, $(CH_3)_2CO$, remain very small due to the lack of efficient gas-phase pathways to these molecules. The high density of the ultracompact core ensures that cosmic-ray ionisation can only produce a low fractional ionisation which thus ensures that the time-scales for processing parent molecules and forming daughter molecules is long. The fractional abundance of molecular ions is low in this region.

3.1.2. The compact core

In this region the gas temperature varies from 190 K at 0.01 pc to about 75 K at 0.1 pc. The evolution of column densities in this component is seen in Fig. 2. The lower gas density ensures that the fractional ionisation is larger here than in the ultracompact core and a more active ion-molecule chemistry can develop here. Since the temperature is lower here, H-atom reactions are not as important and H_2S is not destroyed as rapidly as in the ultracompact core, and after 3000 years it still accounts for about 90% of the total sulphur. The decreasing temperature also allows for a larger abundance of certain atoms and radicals to exist for longer. Examples include C, N, O, OH and NO. The increased OH abundance leads to an increase in the CO_2 abundance through the reaction of CO with OH. After a time of 3-10 $\times 10^3$ years, a number of molecules, including CO_2, H_2CO, O_2, NO, OH and H_2S, have their peak fractional abundances in this component.

3.1.3. The halo

This region, in which the temperature falls to 18 K and the density to $n(H_2) = 816$ cm^{-3} at a radius of 3.5 pc, follows the normal chemistry expected in a dense interstellar cloud, with the main chemical syntheses being driven by ion-neutral and neutral-neutral reactions. The evolution of column densities as a function of time is shown in Fig. 3. Fractional abundances and

column densities of ions have their peak values in this region and allow constraints to be made on the cosmic-ray ionisation rate, ζ. In order to reproduce the observed column density of HCO^+ toward G 34.3, we need to adopt $\zeta = 1.3 \times 10^{-16}$ s^{-1}, a factor of 10 larger than the standard interstellar value. We also adopt this ionisation rate in the compact and ultracompact cores.

3.2. Detailed chemistry

In this subsection, we concentrate on a few typical species and discuss their chemistry in some detail. Comparison between observations and the models is presented in the next section. Figs. 4 - 6 present the radial distributions of many molecules for particular choices for the halo and core ages, while Figs. 7 and 8 present histograms outlining the contribution of each component to the total column density for a number of important species for times corresponding to the data of Tables 5 (3.16×10^3 years in the UCC and CC components and at 10^5 years in the halo) and 6 (10^4 years in the UCC and CC components and at 10^5 years in the halo), which are available only in electronic form.

3.2.1. H_2O

Water is the major component of interstellar ices (Whittet 1993) and has an adopted fractional abundance of 10^{-5} in the grain mantle. Upon evaporation, H_2O is attacked by H atoms, although because of an activation energy of 9720 K, the reaction is slow even in the hot gas in the ultracompact core (Fig. 1). The H_2O parent is destroyed most effectively by proton transfer followed by dissociative recombination. Because the degree of fractional ionisation decreases with increasing density, loss of H_2O by the latter process is very slow in the ultracompact core and the water abundance does not decrease until around 10^4 years and then only in the compact core (Fig. 2), where the lower density ensures a larger fractional ionisation and a more rapid destruction than in the ultracompact core. Indeed at 10^5 years, the H_2O abundance has even increased somewhat in the ultracompact core as oxygen released from parent O_2 gets locked up in water through successive reactions with H_2. In the halo, water formation is initiated by the proton transfer reaction between H_3^+ and atomic oxygen and the water abundance builds up on a time-scale of around 10^5 years, (Fig. 3), although at this time its column density is still an order of magnitude less than that in the compact core at 3000 years and a factor of 30 less than that in the ultracompact core. *Within a factor of 2-3, the gas-phase abundance of H_2O reflects the solid-state abundance of H_2O even at times as long as 3×10^5 years after mantle evaporation.*

3.2.2. O_2

Molecular oxygen is injected from grain mantles at a fractional abundance of 10^{-6}. The proton affinity of O_2 is less than that of H_2 so that proton transfer reactions followed by dissociative recombination do not destroy it. Instead destruction by He^+, and, most importantly in the ultracompact core, reaction with atomic sulphur released in the break-down of H_2S, to form SO, destroys O_2 on a faster time-scale than that of H_2O, some of which is recycled in the dissociative recombination of H_3O^+ (Williams et al. 1996). In the compact core, destruction by C atoms also becomes appreciable although loss by S atoms still dominates. In the halo, O_2 is formed primarily by the neutral reaction between O and OH and destroyed by carbon atoms. The O_2 abundance increases as the abundance of carbon atoms decreases but at 10^5 years is a factor of around six less than the abundance of atomic oxygen.

The breakdown of the parent molecules H_2O and O_2 leads to the presence of the reactive species OH and O in the warm gas and promotes a gas-phase chemistry which enriches the gas in more complex species as will be discussed in what follows.

3.2.3. NH_3 and N_2

Ammonia is often considered to be a major molecule in interstellar molecular ices although it has yet to be detected in an interstellar infrared spectrum. Many hot core sources, such as G 34.3, contain large abundances of NH_3 and it appears that in these sources, much of this abundance must be due to the evaporation of ice mantles. However, it is possible that a high-temperature neutral chemistry can produce NH_3 so that it is *a priori* difficult to determine if the observed gas-phase NH_3 has arisen from the evaporation of grain mantles. A discriminant lies in the observation of NH_2D and, in particular, of the NH_2D/NH_3 abundance ratio. If this ratio is much larger than the cosmic D/H ratio then it is clear evidence of a cold chemistry, and hence formation on grain mantles. NH_3 is destroyed by the usual ion-neutral reactions involving protons and He^+, which dominate in the ultracompact and compact cores (Figs. 1 and 2). Loss by reaction with atomic hydrogen has an activation energy of nearly 5000 K and is slow even in the warmest cores. As a result, time-scales of over 10^4 years are needed to breakdown a significant amount of NH_3. It is also possible that a significant amount of nitrogen could be tied up in grain mantles in the form of N_2 which has no active infrared modes. In our model we adopt a grain mantle fraction abundance of 2×10^{-5}. The N_2 is destroyed by He^+ ions upon evaporation and releases N^+ and N atoms which react further. N^+ reacts with H_2 to initiate an ammonia chemistry (Adams et al. 1984, Yee et al. 1987) while N atoms react with radicals such as OH, C_2, CH_2 and CH_3 to produce NO, CN and HCN, respectively, while the N + SH reaction leads to NS. The N + NO reaction also leads to some reformation of N_2 in the ultracompact core.

In some hot cores, such as W3(H_2O), the NH_3 abundance is low and it is possible that the evaporation of N_2 leads to the observed abundance (Helmich et al. 1997). In the cloud halo, formation of NH_3 is inefficient and high abundances are only reached at late times. In our calculation, this component of the cloud contributes less than one percent of the total column density at an halo age of 10^5 years and a core age of 3000 years (Figs. 4 and 7).

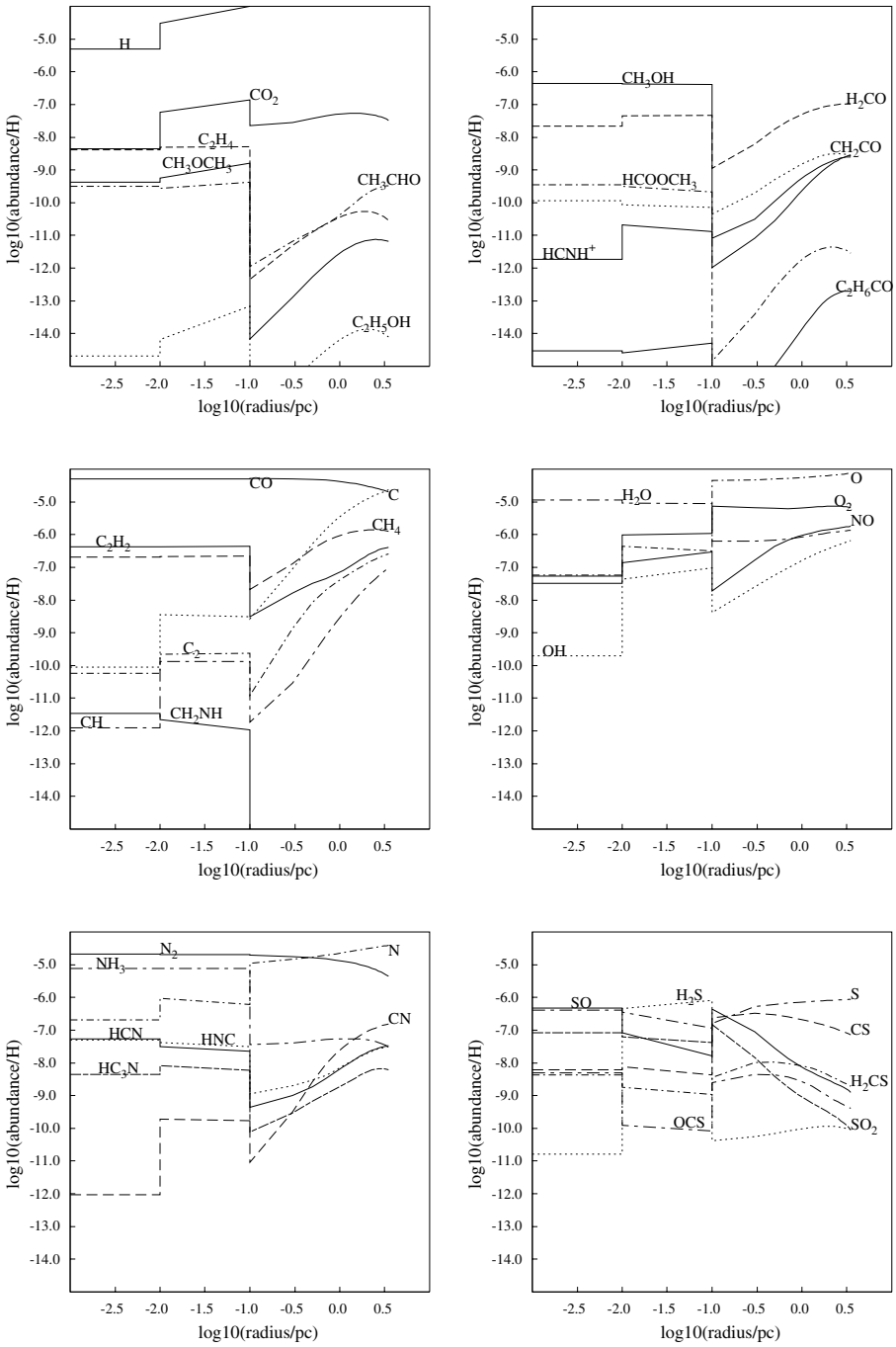

Fig. 4. Radial distributions of fractional abundances at 3.16×10^3 years in the UCC and CC components and at 10^5 years in the halo.

3.2.4. The cyanides

As mentioned previously, CN and HCN form in reactions involving N atoms with simple hydrocarbon molecules. CN also forms in the reaction of C and NO and is destroyed in the ultracompact core by reaction with H_2 to form HCN. At very early times (less than about 1000 years) in the hot cores, the HNC abundance is larger than that of HCN due to the recombination of H_2NC^+ formed in the reaction of C^+ with NH_3. On times longer than 1000 years, the HCN and HNC abundances are roughly equal as a number of neutral-neutral reactions become more efficient at producing HCN, although HCN remains a few times larger in the UCC (Fig. 1). Note that the chemical model did not include destruction of HNC by O atoms although we did include the H + HNC reaction (Talbi et al. 1996). The former process would decrease the HNC abundance in the hot gas. In the halo, HCN and HNC formation occurs through the usual gas-phase routes which produce smaller column densities than in the hot cores.

In hot gas the formation of CH_3CN is driven almost entirely through the radiative association of CH_3^+ with HCN, which is also the major formation mechanism to CH_3CN in the halo. At

a core age of 10^4 yr, the column density of CH_3CN is largest in the ultracompact core, with that in the compact core being a factor of about four smaller and that in the halo smaller by about an order of magnitude (Fig. 8).

The cyanopolyyne molecule, HC_3N, is formed efficiently in hot gas through the neutral reactions of N with C_3H_2 and C_2H_2 with CN, and has approximately equal column densities in both the ultracompact and compact core components. The latter reaction is also responsible for producing HC_3N in the halo but the lower abundance of C_2H_2 in this component leads to a much lower column density, by one to two orders of magnitude. In this regard it is interesting to note that HC_3N is often regarded as a typical cold cloud tracer; these calculations and observations of hot cores, including the detection of vibrationally excited HC_3N, show that the molecule is also formed efficiently in hot gas if C_2H_2 is evaporated from grain mantles.

3.2.5. H_2S

Hydrogen sulphide, H_2S, is assumed to be a product of grain mantle evaporation. While Minh et al. (1991) have observed H_2S in a variety of molecular clouds, there has been no comprehensive survey of H_2S in hot cores, but the $2_{2,0}$ - $2_{1,1}$ transition at 216.71 GHz was detected when searched for in many of the sources investigated by Hatchell et al. (1997). The activation energy barrier for destruction of H_2S by H atoms is small, $\sim$ 350 K, and H_2S is destroyed extremely rapidly in the ultracompact core with a fractional abundance reduced by a factor of two 300 years after evaporation and by around a factor of 50, 1000 years after evaporation (Fig. 1). The slightly lower temperatures in the compact core ensure that H_2S survives for around 10^4 years (Fig. 2). Reaction with atomic hydrogen liberates the SH radical which is also destroyed by H atoms in an activationless reaction. The S atoms created are very reactive and combine with OH and O_2, released from the mantles, to produce SO. A fast reaction between SO and OH produces SO_2 and the end result of the hot gas chemistry is to convert a gas rich in H_2S to one rich in SO and SO_2. Other sulphur containing molecules such as CS, OCS and H_2CS also form in the hot gas but with abundances one to orders of magnitude less than those of SO and SO_2 for times less than 10^4 years. On longer time-scales, SO is destroyed by C atoms to form CS which becomes the most abundant sulphur-bearing molecule after SO_2.

The difficulty of synthesising H_2S in cold gas is well known, and as a result, its abundance always remains small in the halo (Fig. 3). Here atomic sulphur is most abundant. The molecular form of sulphur depends on the age of the halo. For times less than about 10^6 years, CS is the most abundant neutral due to efficient production of hydrocarbon bonds at early times. Over longer times, carbon is progressively tied up in CO, and the number of C atoms and the hydrocarbon abundances fall. Since C atoms also convert SO to CS, the overall result is a decrease in the CS abundance and a rise in those of SO and SO_2.

3.2.6. Large oxygen-bearing molecules

Two main explanations have been proposed to explain the presence of large molecules in hot cores:- (i) the molecules are the direct evaporation products of grain mantles, and (ii) the molecules arise from gas-phase synthesis in warm gas where the reactants are smaller products of mantle evaporation. In the first case, observations of the gas-phase in hot cores can tell us directly about the trace components of the mantles, material which exists in the ice with an abundance too low to be detected directly in infrared absorption. In the second case, the observations may be used to derive the minimum set, and abundances, of the small molecules in the mantles. These may include species, such as O_2 and N_2, which are unobservable in the infrared. In both cases, the observations and interpretation may be used to constrain models of solid-state chemical evolution of the ices. However, it is important to note that a third possibility exists, namely that our knowledge of the gas-phase chemistry of these large molecules is simply incomplete and that grain surface chemistry is not needed, at least in the sense implied by (i).

In the present calculations, we investigate proposal (ii). Ethanol, C_2H_5OH, is formed in the dissociative recombination of $C_2H_5OH_2^+$ formed in the reaction of H_3O^+ and evaporated C_2H_4, whilst its isomer $(CH_3)_2O$ is formed via the reaction of CH_3OH and $CH_3OH_2^+$. $(CH_3)_2O$ is the more abundant species because its formation involves more abundant reactants, at least with the assumption of a large CH_3OH abundance evaporated from grain mantles. Such an assumption appears reasonable given the recent interferometer observations of CH_3OH (Mehringer & Synder 1996).

Methyl formate, $HCOOCH_3$, is also formed efficiently in the hot gas via the reaction of $CH_3OH_2^+$ with H_2CO followed by dissociative recombination and has a column density of about 10^{14} cm^{-2} after 3000 years in both the ultracompact and compact cores.

Acetaldehyde, CH_3CHO, is produced in the ultracompact core mainly through the neutral-neutral reaction of O atoms and C_2H_5, which has a fast rate coefficient of 1.33×10^{-10} cm^3 s^{-1} (Tsang & Hampson 1986). The ethyl radical, C_2H_5, is produced following proton transfer reactions with C_2H_6 evaporated from the dust, followed by dissociative recombination. In the compact core, this reaction becomes much less important and CH_3CHO is formed in the recombination of CH_3CHOH^+, which is assumed to be produced in the reaction of $CH_3OH_2^+$ with H_2CO (Millar et al. 1991), although this has yet to be studied in the laboratory.

Acetone, $(CH_3)_2CO$, is the largest oxygen-bearing molecule detected in the interstellar medium and is formed by the reaction between CH_3^+ and CH_3CHO followed by dissociative recombination in both warm and cold gas, but the amount formed is much smaller than that observed in molecular clouds.

3.3. Observed column densities

Despite the wealth of lines detected in G 34.3+0.15 in the 330 - 360 GHz spectral scan (Paper I), column densities are not well

determined for many species as yet. Paper I presented rotation diagrams for around a dozen species and led to estimates of rotation temperature, $T_{\rm rot}$, and beam-averaged column density along the line of sight, where $T_{\rm rot}$ may be used to identify the particular component from which emission arises. However, to be useful, several transitions of a particular molecule must be observed. This restricts the species analysed to be either large or non-linear. In addition, the rotation diagram method assumes that the emission is optically thin - in essence the species should not be very abundant - otherwise $T_{\rm rot}$ is overestimated and the column density underestimated. For example, detailed analysis of CH_3CN emission towards several hot cores (Olmi et al. 1996; Hatchell et al. 1997) indicate that the low K lines are very optically thick and imply that source sizes are on the order of a few arcseconds, much smaller than the beam size at the JCMT, and that column densities may be up to 100 times larger than inferred from the rotation diagram method. It is likely that CH_3OH is also optically thick. For such species, an independent estimate of column density may be obtained by observing an optically thin, isotopic variant, although line blending can often complicate the analysis. Observations of CH_3OH with BIMA at a resolution of $13\,''\times 8\,''$ by Mehringer & Snyder (1996) give $N(CH_3OH) \sim 2\times 10^{17}$ cm^{-2}.

For simple linear molecules, such as CS, HCO^+, HCN and HNC, the spectral scan detects one transition and only a lower limit on the column density can be obtained (Paper I). The detection of isotopic variants often indicates that the main isotope is optically thick. For the purposes of comparison with observation, we have calculated column densities from isotopes where available, using, for example, $H^{13}CN$, $HN^{13}C$, $H^{13}CO^+$, $O^{13}CS$ and $H_2^{13}CO$ (assuming $^{12}C/^{13}C = 60$), $C^{34}S$, $OC^{34}S$ (assuming $^{32}S/^{34}S = 18$) and $C^{17}O$ (assuming $^{16}O/^{17}O = 2400$). We note that the column density of HNC is poorly determined because it rests upon our correct identification of a line at 348.344 GHz as the J=4-3 transition of $HN^{13}C$, which actually lies at a rest frequency of 348.340 GHz. Instead this feature could be due, in whole or in part, to the $40_{2,39}$-$39_{2,38}$ transition of C_2H_5CN which has a frequency of 348.344 GHz. In this case, the derived column density for HNC is an upper limit.

The most accurate estimates for column densities come from multi-transitional studies and we have used these for NH_3 (Heaton et al. 1989), CI (Little at al. 1994), CS (Hauschildt et al. 1995) and HCO^+ (Heaton et al. 1993). Table 4 summarises the observational molecular abundance data for G 34.3.

Because of the current lack of accurate abundances, future observational work should concentrate on spectral scans at other frequencies to constrain column densities of the small, linear molecules, and on scans at offset positions to better separate the contributions from each of the cloud components.

Table 4. Column densities estimated from observation.

Species	N(mol) (cm^{-2})	Notes
CO	>2.9(19)	from $C^{17}O$ (Paper I)
NO	>5.8(15)	(Paper I)
HNC	<3.3(14)	from $HN^{13}C$ (but see Sect. 3.3)
HCO	>5.3(13)	(core)
	>1.2(13)	(halo) (Paper I)
H_2O	1.3(19)	from $H_2^{18}O$ (Gensheimer et al. 1996)
H_2CO	>2.3(16)	from $H_2^{13}CO$
HC_3N	>2.5(13)	from $H^{13}CCCN$ (Paper I)
CH_3C_2H	1.8(16)	(Paper I)
CN	>5.9(14)	(Paper I)
HCN	>9(14)	from $H^{13}CN$
	1.2(15)	from $HC^{15}N$ (Millar, unpublished)
CH_2CO	6.7(14)	(Paper I)
CCH	>8.1(15)	(Paper I)
NH_3	>2.7(18)	from Heaton et al. 1989
CH_3CN	2.4(14)	(Paper I)
	5.7(16)	from Hatchell et al. 1997
CH_3OH	3.7(16)	(core, from Paper I)
	2.6(15)	(halo, from $^{13}CH_3OH$)
	2(17)	from Mehringer & Synder 1996
HCO^+	>7.2(14)	from $H^{13}CO^+$
	>2.0(15)	from $HC^{18}O^+$
H_2S	>1.1(16)	from HDS
		(assuming H_2S/HDS = 100, Paper I)
HCS^+	>3.0(13)	(Paper I)
CS	>3.8(15)	from $C^{33}S$
	>1.2(15)	from $C^{34}S$ (Paper I)
	1.0(16)	from $C^{34}S$ (Hauschildt et al. 1995)
SO	9.1(14)	(halo, from Paper I)
	>2.4(15)	from ^{34}SO (Paper I)
SO_2	2.5(15)	(core)
	1.6(16)	(core, from $^{34}SO_2$)
	1.3(15)	(halo) Paper I
OCS	>1.3(15)	(core)
	>2.9(16)	from $O^{13}CS$
	>7.7(15)	from $OC^{34}S$
H_2CS	1.2(15)	(core)
	>1.9(16)	from $H_2^{13}CS$
	>5.6(16)	from $H_2C^{34}S$; Paper I
NS	>4.0(13)	(Paper I)
C_2H_5OH	3.5(15)	(Paper I)
$HCOOCH_3$	1.6(16)	($T_{\rm rot}$= 150 K, Paper I)

3.4. Particular models

Fig. 4 and Table 5 (available in electronic form) show the results of a time and depth-dependent model for a time of 3000 years in the hot core components and 10^5 years in the halo for a range of species. Fig. 4 shows how fractional abundances with respect to H_2 vary with radial distance through the cloud and Table 5 presents column densities calculated for each component and the total column density for comparison with that observed. The results of Table 5 are summarised in Figs. 7 and 8 which present histograms of calculated column densities for a number of important species broken down by cloud component.

Hot core timescales of more than 1000 yrs are needed to explain the observations of specific molecules. A sensitive indicator of age is the H_2S/SO_2 abundance ratio (Charnley 1997). In order to ensure $N(SO_2) > 10^{16}$ cm^{-2} in the hot core (from

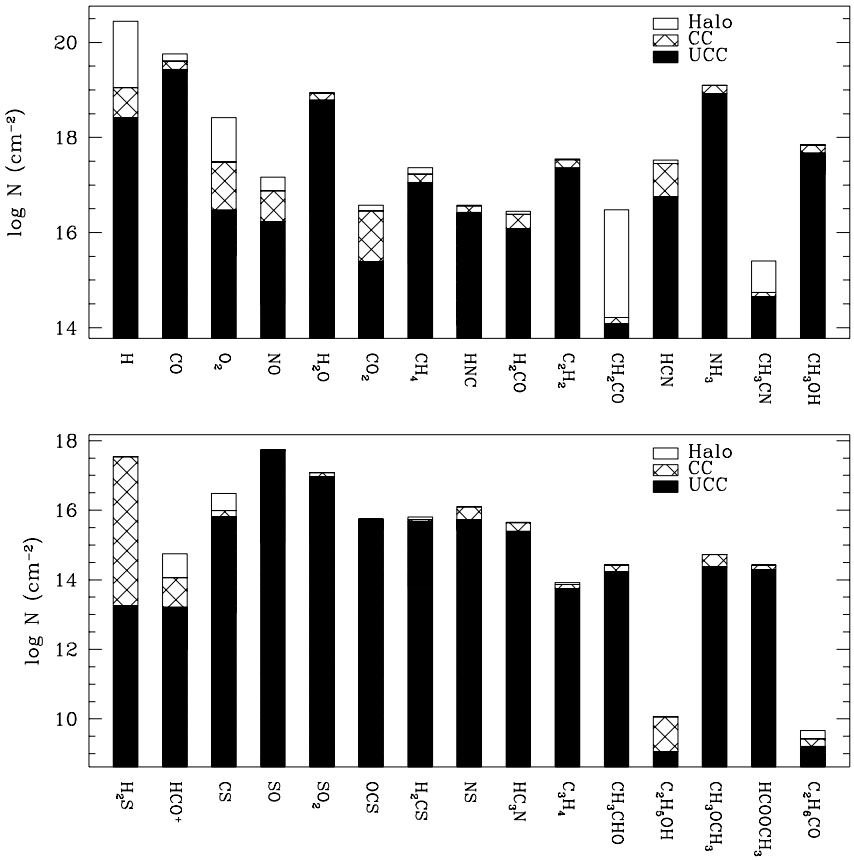

Fig. 7. Histogram of the contribution that the various components make to the column density of selected molecules at a core age of 3 10^3 yrs and a halo age of 10^5 yrs.

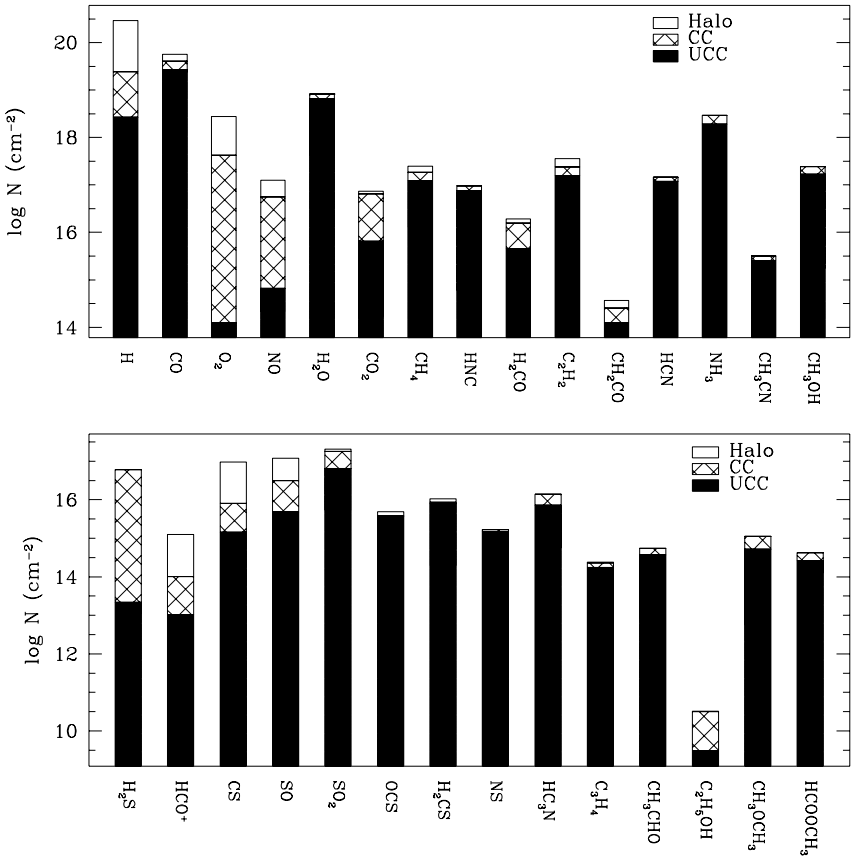

Fig. 8. Histogram of the contribution that the various components make to the column density of selected molecules at a core age of 10^4 yrs and a halo age of 10^5 yrs.

$^{34}SO_2$ with $T_{\rm rot}$ = 130 K, Paper I), we require mantles to have evaporated at least 1000 yrs ago. For $t_{\rm core}$ = 3000 yrs (Figs. 1 and 7, Table 5), the H_2S in the ultracompact core has been reduced from an initial column density of 2.7 $\times 10^{17}$ cm^{-2} to 8.9 $\times 10^{12}$ cm^{-2}. However, the lower gas kinetic temperature in the compact core allows H_2S to survive, with a column density of 1.7 $\times 10^{17}$ cm^{-2}, compared to the (uncertain) observed lower limit of 1.1 $\times 10^{16}$ cm^{-2}. For $t_{\rm core} > 10^4$ yrs, the column density of H_2S falls far below that observed and this provides an upper limit for the age of the hot gas in G 34.3 (Figs. 1 and 2).

The detection of vibrationally excited transitions from CS (Hauschildt et al. 1995), HCN (Paper I) and CH_3CN (Paper I) indicates that infrared pumping plays a major role in the excitation of some species. Detailed models show that such pumping is effective over small angular extents, on the order of a few arcseconds (see, for example, the discussion by Magnum & Wootten 1993), so that emission from vibrationally excited molecules likely arises in the ultracompact core. Since none of the above molecules is assumed to be evaporated from mantles, they also provide a timescale for the hot core phase. HCN is produced very rapidly and abundantly in the hot gas so that it does not give any useful timescales. CS reaches a peak abundance at around 3000 yrs after evaporation begins, before reducing on longer timescales as it is processed into SO and SO_2 (Fig. 1). Methyl cyanide, CH_3CN, is formed on a longer timescale than CS and reaches a column density of around 3 $\times 10^{15}$ cm^{-2} in the ultracompact core at $t_{\rm core} = 10^4$ yrs (Figs 1 and 8). However, this is much lower than the observed value of $\sim 6 \times 10^{16}$ cm^{-2} for a source size of ~ 2 arcseconds (Hatchell et al. 1997). Such a large column density corresponds to a fractional abundance of around 10^{-7} in the ultracompact core. It is very difficult to synthesise this amount of CH_3CN from evaporated N_2 and NH_3 in a physically reasonable timescale and, if correct, implies that CH_3CN must also be evaporated from grains.

Cyanoacetylene, HC_3N, is effectively produced in the hot gas through reaction of evaporated C_2H_2 and CN and is present in an abundance consistent with the detection of vibrationally excited HC_3N in many hot core sources. The larger cyanopolyynes are not formed in abundance in hot gas - N(HC_5N) $< 10^{12}$ cm^{-2} in both the ultracompact and compact cores - since we have assumed that the mantle does not contain highly unsaturated hydrocarbons such as C_4H_2.

Propyne, CH_3C_2H, is produced in both hot and cold gas. Paper I determined N(CH_3C_2H) = 1.8 $\times 10^{16}$ cm^{-2} and $T_{\rm rot}$ = 93 $\pm$ 66 K. Thompson et al. (1997) have observed propyne at offset positions in a number of hot cores in order to separate core/halo contributions. For G 34.3, they find N(CH_3C_2H) = 4.6 $\times 10^{14}$ cm^{-2} and $T_{\rm rot}$ = 37 K at (0, 20) compared to N(CH_3C_2H) = 1.2 $\times 10^{15}$ cm^{-2} and $T_{\rm rot}$ = 95 K at (0,0), where the offset positions are given in arcseconds. Note that the latter column density is about an order of magnitude less than that given in Paper I. Assuming that N(CH_3C_2H) $\sim 7 \times 10^{14}$ cm^{-2} arises in the ultracompact and compact core components, a better fit occurs for $t_{\rm core} \sim 10^4$ yrs, when the total column density of CH_3C_2H in the two hot components is $\sim 2.3 \times 10^{14}$ cm^{-2}(Fig. 8). The maximum value of N(CH_3C_2H) in the halo is $\sim 6 \times 10^{14}$ cm^{-2} at $t_{\rm halo} \sim$ a few $\times 10^4$ yrs. We note that a halo age of $\sim 10^6$ yrs is incompatible with the observed column densities. Hydrocarbon molecules, such as propyne, and others, such as CH_3OH - inferred in the halo from observations of $^{13}CH_3OH$ (Paper I) - have low abundances at long times. For example, at $t_{\rm halo} = 10^6$ yrs, we find halo column densities of 3.5 $\times 10^{13}$, 6.5 $\times 10^{11}$, 5.5 $\times 10^9$, and 1.8 $\times 10^{12}$ cm^{-2} for C_2H, HC_3N, CH_3C_2H and CH_3OH, respectively (see Fig. 6).

Sulphur chemistry shows some interesting differences between hot and cold gas. At early times in hot gas, the dominant molecule, once H_2S has been destroyed, is SO, followed by SO_2 and CS - see the entries under UCC in Fig. 7. As $t_{\rm core}$ increases, SO_2 is synthesised more efficiently and the order is N(SO_2) $>$ N(SO) $>$ N(CS). This relationship holds in both the ultracompact and compact cores at $t_{\rm core} = 10^4$ yrs (see Fig. 8).

Chemical evolution occurs differently in the halo. At early times, i.e., $t_{\rm halo} < 10^5$ yrs, the most abundant molecule is CS, followed by SO and SO_2, with a major fraction of sulphur being in atomic form (Fig. 3). This is due to the large abundance of simple hydrocarbon molecules at early times. As the halo gas evolves chemically, carbon is tied up in CO. This removes reactive carbon from the gas and causes a rise in O_2, which causes SO to be more abundant than CS for $t_{\rm halo} > 10^5$yrs. The abundance of HCS^+ follows that of CS and most of its column density arises in the halo. The lack of protonated molecules in the hot, dense cores ensures that the HCS^+/CS abundance ratio is $\sim 10^{-4}$ there, but $\sim 10^{-2}$ or larger in the cooler, halo gas.

The abundances of the large, oxygen-bearing molecules generally increase in the hot gas as $t_{\rm core}$ increases to 10^4 yrs, and decrease in the halo gas for $t_{\rm halo} >$ few $\times 10^5$ yrs. Figs. 1-3 and 8 shows that, even with the optimum choice of $t_{\rm core}$ and $t_{\rm halo}$, the calculated abundances of ethanol, C_2H_5OH, and methyl formate, $HCOOCH_3$, are $\sim 10^5$ and 10^2 times smaller respectively than the observed column densities. Furthermore, the column density of dimethyl ether, $(CH_3)_2O$, reaches a maximum value of 10^{15} cm^{-2}, almost all of which arises in the hot gas, whilst that of acetone, $(CH_3)_2CO$, reaches a maximum of only 10^{10} cm^{-2}. The abundance of $(CH_3)_2O$ is consistent with its detection in G 34.3 (Paper I), although it was not possible to estimate its abundance there, and in other hot cores with an abundance similar to that of C_2H_5OH. Acetaldehyde, CH_3CHO, is calculated to have a column density of 5 $\times 10^{14}$ cm^{-2} at $t_{\rm core} = 10^4$ yrs in the hot gas (Figs. 1 and 8) and may be detectable.

The abundance of C_2H_5OH is so much less than the observed column density in G 34.3 that it will be difficult to find any efficient gas-phase synthesis. Such a synthesis will need to involve abundant oxygen-bearing species, such as OH and OI, and probably involve neutral-neutral chemistry as the ionisation fraction in the dense, hot gas in G 34.3 is small. If such a production mechanism cannot be identified, it will imply that ethanol is made on grain surfaces (Millar et al. 1995). Charnley et al. (1995) have investigated the implications of the surface formation of alcohols and concluded that some very large species can be formed in the hot gas following alcohol release to the gas. Searches for such molecules together with interferometric ob-

servations to look for spatial correlations between molecules are important tests of this model.

4. Conclusions

We have investigated a time-dependent chemical kinetic model for the molecular cloud associated with the UCHII region G 34.3+0.15. Because the physical conditions and chemical composition of this cloud have been determined by both multi-transitional observations and a submillimetre spectral scan, we have been able to construct a detailed physical and chemical model of the cloud. We have followed the chemical evolution at each of 22 radial points in the cloud over a timescale of 10^8 yrs. In the cloud halo, we have started from atoms (except for H_2), whilst in the two hot central components - the ultracompact and compact cores - the initial abundances are given by assuming that a molecular ice has been evaporated. Different combinations of time in the halo, $t_{\rm halo}$, and in the core, $t_{\rm core}$, have been used to plot fractional abundances and calculate column densities in each of the three components.

While the model is an order of magnitude more computationally intensive than previous hot core calculations, it is disappointing that it has not been better constrained by observations. In part this is due to the lack of accurate column densities for many small, linear molecules for which multitransition studies of their main isotopic variants are needed, and in part because emission from many complex molecules, such as CH_3CN and CH_3OH, is optically thick. This precludes any easy determination of rotation temperatures and column densities from rotation diagrams. In addition, most observations of hot cores have been with single dish telescopes which provide column densities beam-averaged on scales of 10-20 arcseconds, typically. Interferometric and modified rotation diagram techniques (Olmi et al. 1996; Hofner et al. 1996; Hatchell et al. 1997) indicate that, for some species, source sizes may be an order of magnitude smaller and abundances much larger than estimated from single dish measurements. It is also worth pointing out that measurements integrate along the line-of-sight. Toward G 34.3, we have evidence, all of which agrees in general terms, of the actual radial structure of the cloud. Even so, it is difficult to separate out core/halo contributions to the emission. Studies at offset positions are needed to do this properly. Finally, the H_2 column densities toward many hot cores are uncertain. The advent of SCUBA on the JCMT will allow determinations of these through observations of the dust continuum radiation.

Despite these caveats, comparison with observation shows that $t_{\rm halo}$ is probably less than about 10^6 yrs old, otherwise the abundances of molecules such as CH_3C_2H and CH_3OH, become too small as an increasing amount of carbon is processed into CO. The preferred age for the hot core of G 34.3 is around 3000 to 10^4 yrs. For times less than 1000 yrs, H_2S is not destroyed and the abundances of molecules such as CS, SO and SO_2 fall below those observed. The detection of vibrationally excited CS (Hauschildt et al. 1995) indicates that there is an appreciable column density of CS in the ultracompact core.

The calculations show that molecules traditionally associated with cold gas can have large abundances in hot cores. These include HC_3N, from which vibrationally excited emission is seen, C_2H and CH_3C_2H. Such molecules are probably daughter products formed when simple parent molecules evaporate from the grains.

Not all complex molecules appear to be daughter species. Whilst $(CH_3)_2O$ probably is a daughter, the large abundances of C_2H_5OH (Millar et al. 1995) and CH_3CN (Olmi et al. 1996; Hatchell et al. 1997) indicate that these may have been formed on grain mantles. If CH_3CN is a parent, it may indicate that ethyl cyanide, C_2H_5CN, whose presence in G 34.3 has been confirmed by the interferometer observations of Mehringer & Synder (1996), may also be synthesised on grains. An observational test for parent/daughter species would be to investigate the variations in molecular abundances for a wide range of hot core sources. On timescales approaching 10^4 yrs, parent abundances are fairly insensitive to time while those of daughters vary greatly.

The model outlined here does a reasonable job at explaining the observed column densities toward G 34.3 and it certainly appears to be the case that the evaporation of grain mantles has played a central role in determining the gas-phase composition of the hot gas in G 34.3 (see also Mehringer & Snyder 1996). More refined chemical models should take into account the possibility that the mantle composition varies with radial distance so that different molecules may evaporate at different distances. Such a model may help explain the different gas/solid abundance ratios detected towards low-mass star-forming regions with *ISO* (van Dishoeck et al. 1996).

Acknowledgements. The work of TJM is supported via a grant from the Particle Physics and Astronomy Research Council (PPARC). We are grateful to the referee, Peter Schilke, for helpful comments.

References

Adams, N. G., Smith, D., Millar, T. J., 1984, MNRAS, 211, 857.
Brown, P.D., Charnley, S.B., Millar, T.J., 1988, MNRAS, 231, 409.
Brown, P.D., Millar, T.J., 1989a, MNRAS, 237, 661.
Brown, P.D., Millar, T.J., 1989b, MNRAS, 240, 25P.
Caselli, P., Hasegawa, T. I., Herbst, E., 1993, ApJ, 405, 548.
Charnley, S.B., 1997, ApJ, 481, 396.
Charnley, S. B., Kress, M. E., Tielens, A. G. G. M., Millar, T. J., 1995, ApJ, 448, 232.
Charnley, S. B., Millar, T. J., 1994, MNRAS, 270, 570.
Charnley, S. B., Tielens, A. G. G. M., Millar, T. J., 1992, ApJ, 399, L71.
Gensheimer, P., Mauersberger, R., Wilson, T.L. 1996, A&A, 314, 281.
Hatchell, J. et al. 1997, A&A, in prep.
Hauschildt, H., Güsten, R., Schilke, P., 1995, in *The Physics and Chemistry of Interstellar Molecular Clouds*, eds. G. Winnewisser & G.C. Pelz, Springer Verlag, Berlin, p. 52.
Heaton, B. D., Little, L. T., Bishop, I.S., 1989, A&A, 213, 148.
Heaton, B. D., Little, L. T., Yamashita, T., Davies, S. R., Cunningham, C. T., Monteiro, T. S., 1993, A&A, 278, 238.
Helmich, F. P., van Dishoeck, E. F., 1997, ApJS, in press.
Helmich, F.P., Millar, T. J., van Dishoeck, E.F., 1997, A&A, in prep.

Hofner, P., Kurtz, S., Churchwell, E., Walmsley, C. M., Cesaroni, R., 1996, ApJ, 460, 359.
Little, L. T., Gibb, A. G., Heaton, B. D., Ellison, B. N., Claude, S. M. X., 1994, MNRAS, 271, 649.
Macdonald, G.H., Gibb, A.G., Habing, R.J., Millar, T.J., 1996, A&AS, 119, 333.
MacKay, D. D. S., 1995, MNRAS, 274, 694.
Magnum, J. G., Wootten, A., 1993, ApJS, 89, 123.
Mallard, W. G., Westley, F., Herron, J. T., Hampson, R. F., Frizell, D. H., 1994, *NIST Chemical Kinetics Database: Ver. 6.0,* National Institute of Standards and Technology, Gaithersburg, MD.
Mehringer, D. M., Snyder, L. E., 1996, ApJ, 471, 897.
Minh, Y. C., Ziurys, L. M., Irvine, W. M., McGonagle, D., 1991, ApJ, 366, 192.
Millar, T. J., Herbst, E., Charnley, S. B., 1991, ApJ, 369, 147.
Millar T.J., Macdonald G.H., Habing R.J., 1995, MNRAS, 273, 25.
Olmi, L., Cesaroni, R., and Walmsley, C. M., 1996, A&A, 307, 599.
Rodgers, S. D., Millar, T. J., 1996, MNRAS, 280, 1046.
Sutton, E. C., Jaminet, P. A., Danchi, W. C., Blake, G. A., 1991, ApJS, 77, 255.
Sutton, E. C., Peng, R., Danchi, W. C., Jaminet, P. A., Sandell, G., Russell, A. P. G., 1995, ApJS, 97, 455.
Talbi, D., Ellinger, Y., Herbst, E., 1996, A&A, 314, 688.
Thompson, M., et al. 1997, A&A, in prep.
Tsang, W., Hampson, R. F., 1986, J. Phys. Chem. Ref. Data, 15, 1087.
Turner, B. E., 1991, ApJS, 76, 617.
van Dishoeck, E. F., et al., 1996, A&A, 315, L349.
Whittet, D. C. B., 1993, in *Dust and Chemistry in Astronomy,* eds. T. J. Millar & D. A. Williams, IoP Publishers, Bristol, p. 9.
Williams, T. L., Adams, N. G., Babcock, L. M., Herd, C. L., Geoghegan, M., 1996, MNRAS, 282, 413.
Yee, J. H., Lepp, S., Dalgarno, A., 1987, MNRAS, 227, 461.

This article was processed by the author using Springer-Verlag LaTeX A&A style file *L-AA* version 3.